1 **Title: Ammonium recycling supports toxic *Planktothrix* blooms in Sandusky Bay, Lake**
2 **Erie: evidence from stable isotope and metatranscriptome data**
3
4
5 Justyna J. Hampel[a*], Mark J. McCarthy[a], Michelle Neudeck[b], George S. Bullerjahn[b], Robert
6 Michael L. McKay[b], and Silvia E. Newell[a]
7
8 [a] Department of Earth & Environmental Sciences, Wright State University, Dayton, OH, United
9 States
10 [b] Department of Biological Sciences, Bowling Green State University, Bowling Green, OH,
11 United States
12 [*] Corresponding author (hampel.4@wright.edu)
13
14

15   **Abstract:**

16   Sandusky Bay, Lake Erie, receives high nutrient loadings (nitrogen and phosphorus) from the

17   Sandusky River, which drains an agricultural watershed. Eutrophication and cyanobacterial

18   harmful algal blooms (cyanoHABs) persist throughout summer. *Planktothrix agardhii* is the

19   dominant bloom-forming species and the main producer of microcystins in Sandusky Bay. Non-

20   N_2 fixing cyanobacteria, such as *Planktothrix* and *Microcystis*, thrive on chemically reduced

21   forms of nitrogen, such as ammonium (NH_4^+) and urea. Ammonium regeneration and potential

22   uptake rates and total microbial community demand for NH_4^+ were quantified in Sandusky Bay.

23   Potential NH_4^+ uptake rates in the light increased from June to August at all stations. Dark uptake

24   rates also increased seasonally and, by the end of August, were on par with light uptake rates.

25   Regeneration rates followed a similar pattern and were significantly higher in August than June.

26   Ammonium uptake kinetics during a *Planktothrix*-dominated bloom in Sandusky Bay and a

27   *Microcystis*-dominated bloom in Maumee Bay were also compared. The highest half saturation

28   constant (K_m) in Sandusky Bay was measured in June and decreased throughout the season. In

29   contrast, K_m values in Maumee Bay were lowest at the beginning of summer and increased in

30   October. A significant increase in V_{max} in Sandusky Bay was observed between July and the end

31   of August, reflective of intense competition for depleted NH_4^+. Metatranscriptome results from

32   Sandusky Bay show a shift from cyanophycin synthetase (luxury NH_4^+ uptake; *cphA1*)

33   expression in early summer to cyanophycinase (intracellular N mobilization; *cphB/cphA2*)

34   expression in August, supporting the interpretation that the microbial community is nitrogen-

35   starved in late summer. Combined, our results show that, in late summer, when nitrogen

36   concentrations are low, cyanoHABs in Sandusky Bay rely on regenerated NH_4^+ to support

37   growth and toxin production. Increased dark NH_4^+ uptake late in summer suggests an important

38   heterotrophic contribution to NH_4^+ depletion in the phycosphere. Kinetic experiments in the two

39   bays suggest a competitive advantage for *Planktothrix* over *Microcystis* in Sandusky Bay due to

40   its higher affinity for NH_4^+ at low concentrations.

41
42   **Keywords:** Nitrogen, cyanobacteria, *Planktothrix*, nutrient management, Lake Erie, Sandusky
43   Bay
44
45
46
47
48
49
50
51
52
53
54
55
56
57
58
59
60

61 **1. Introduction**

62

63   Lake Erie, the shallowest and most productive of the Laurentian Great Lakes, provides

64 key ecosystem services and supports an annual US$50 billion tourism, fisheries, and boating

65 industry (Watson et al., 2016). However, Lake Erie has been subjected to eutrophication, habitat

66 loss, impoundments, and introduction of invasive species. The western basin of Lake Erie is

67 particularly susceptible to eutrophication and cyanobacterial harmful algal blooms (cyanoHABs),

68 which have increased since the mid-1990's, threatening its ability to provide ecosystem services

69 (Watson et al., 2016). In the 1960's and 1970's, cyanoHABs in Lake Erie consisted mostly of

70 nitrogen (N) fixing taxa (e.g., *Dolichospermum,* [*formerly Anabaena*]*,* and *Aphanizomenon*).

71 However, upon re-eutrophication in the 1990's, cyanoHABs shifted to mostly non-N_2 fixing taxa

72 (Steffen et al., 2014; Watson et al., 2014; Chaffin et al., 2018). CyanoHABs in the western basin

73 are related to increased N and phosphorus (P) loadings from the Maumee River, which carries

74 runoff from a primarily agricultural watershed (Richards et al., 2010). In Maumee Bay, non-

75 diazotrophic *Microcystis aeruginosa* is the dominant bloom organism, a common cyanoHAB

76 species found globally (Havens et al., 2001; McCarthy et al., 2009; Kurmayer et al., 2015).

77 However, blooms in Sandusky Bay, east of the western basin, are almost entirely attributed to the

78 filamentous, non-N_2 fixing *Planktothrix agardhii* (Davis et al., 2015; Salk et al., 2018). *P.*

79 *agardhii* has a wide distribution and is ubiquitous in eutrophic lakes globally (Suda et al., 2002;

80 Steffen et al., 2014; Kurmayer et al., 2015).

81   Sandusky Bay is a shallow basin, formed from a drowned river mouth (mean depth = 2.6

82 m; area = 162 km^2) in the southern part of Lake Erie (Fig 1; Conroy et al., 2007). Sandusky Bay

83 receives high N and P loadings from the Sandusky River, which also flows through primarily

84 agricultural areas (Conroy et al. 2007; Richards et al. 2010). The residence time in Sandusky Bay

85   can vary from 8 to 81 days (Salk et al., 2018) and is similar to the residence time in Maumee Bay

86   and the western basin (51 days; Millie et al., 2009). Total N concentrations in the bay decrease as

87   the summer bloom progresses, starting with high concentrations of dissolved inorganic nitrogen

88   (DIN) in June and July (50–600 µM), followed by low (<5 µM) to undetectable DIN

89   concentrations in August–October, mainly due to a decrease in NO_3^- (Davis et al., 2015; Salk et

90   al., 2018). These low N concentrations by the end of summer, and elevated, albeit variable

91   concentrations of soluble reactive phosphorus (SRP; Davis et al., 2015; Salk et al., 2018),

92   suggest seasonal N limitation in Sandusky Bay. Nutrient addition experiments showed that both

93   bloom growth and microcystins (MC) production were stimulated by additions of dissolved N,

94   but not P, and that additions of both $NH_4^+ + PO_4^{3-}$ and urea + PO_4^{3-} yielded highest MC

95   concentrations (Davis et al., 2015). High ambient N concentrations are required for the

96   production of microcystins, which contain 10 N atoms per microcystin molecule (Davis et al.,

97   2015; Gobler et al., 2016). Another study from Sandusky Bay also showed growth stimulation by

98   NH_4^+, NO_3^-, and urea, consistent with N limitation in the system (Chaffin and Bridgeman, 2014).

99   These results emphasize the importance of chemically reduced N species during cyanoHABs

100   (Glibert et al., 2016).

101   Comprehensive phytoplankton community studies in Sandusky Bay show that *P.*

102   *agardhii* is the dominant species during the bloom season and the main producer of MC (Rinta-

103   Kanto and Wilhelm 2006; Conroy et al., 2007; Davis et al., 2015; Steffen et al., 2015; Salk et al.,

104   2018). *P. agardhii* may proliferate in these waters due to its tolerance to a broad temperature

105   range and acclimation to growth at low light intensity (Oberhaus et al., 2007). The shallow depth

106   of Sandusky Bay leads to suspended sediment particles that create turbidity and low light

107   conditions, where *Planktothrix* thrives (Scheffer 1997). Additionally, *Planktothrix* is common in

108   lakes with low bioavailable N and low N:P (Rücker et al., 1997), conditions that prevail in

109   Sandusky Bay in late summer. However, these low N:P conditions are often caused by the

110   cyanoHABs (e.g., Xie et al. 2003), and this pattern of DIN depletion occurring after bloom

111   initiation has been observed in Sandusky Bay (Chaffin and Bridgeman, 2014; Davis et al., 2015;

112   Salk et al., 2018). Once low N:P conditions are established, *P. agardhii* has a low half-saturation

113   constant (K_m) for NH_4^+ (Zevenboom and Mur 1981), and thus high substrate affinity, compared

114   to other non-diazotrophic cyanobacteria, e.g., *Microcystis* (Niklisch and Khol 1983). This high

115   affinity, along with high maximum uptake rates (V_{max}; Zevenboom et al., 1980), makes

116   *Planktothrix* an excellent competitor for N substrate in low N conditions.

117   Non-diazotrophs, such as *Microcystis* and *Planktothrix*, are highly competitive for

118   chemically reduced N forms, such as NH_4^+ and urea (Blomqvist et al., 1994; Glibert et al., 2016).

119   NH_4^+ transport across the cell membrane, via ammonia transporters (*amt* genes), and assimilation

120   into biomass, via the glutamine synthetase pathway (*gln* genes), are less energy intensive than for

121   NO_3^- (Glibert et al., 2016). During high *in situ* DIN conditions, cyanobacteria can assimilate and

122   store N intracellularly (luxury uptake) to use when DIN is depleted. Cyanobacteria including,

123   *Planktothrix* spp., are capable of synthesizing cyanophycin granules as an N storage polymer

124   (Van de Waal et al., 2010) when N is bioavailable, and synthesis of cyanophycin is dependent on

125   cyanophycin synthetase, encoded by *cphA1*. Degradation of cyanophycin is a function encoded

126   by *cphB,* cyanophycinase, and is co-transcribed with another cyanophycinase gene, *cphA2*, in the

127   *cphBA2* operon**.** Cyanophycinase mobilizes stored N when DIN in the water column is depleted.

128   Due to high biological demand and fast turnover rates, NH_4^+ rarely accumulates in the

129   water column, resulting in low *in situ* concentrations. Thus, NH_4^+ dynamics and turnover rates

130   are important components of the aquatic N cycle and productivity in eutrophic lakes affected by

131 cyanoHABs. Regeneration of NH_4^+ contributes to internal cycling and availability of NH_4^+ for

132 assimilation (James et al., 2011; Paerl et al., 2011; McCarthy et al., 2013). For example, rapid

133 NH_4^+ turnover can fuel and sustain blooms, despite low *in situ* NH_4^+ concentrations (Paerl et al.,

134 2011; McCarthy et al., 2013; Hampel et al., 2018). On the other hand, cyanobacteria must

135 compete with other organisms for NH_4^+; for example, nitrifiers are an important link between

136 reduced N in the water column and its subsequent removal through denitrification (An and Joye,

137 2001). Studies that focus solely on monitoring static nutrient concentrations can miss important

138 aspects of nutrient and cyanoHAB dynamics. Therefore, spatio-temporal NH_4^+ cycling, rather

139 than *in situ* NH_4^+ concentration, can provide better insights into understanding the dominance of

140 non-N_2 fixing cyanoHABs (Hampel et al., 2018).

141   Little is known about NH_4^+ uptake and regeneration and the kinetics of NH_4^+ uptake

142 during *Planktothrix* blooms. Light availability is likely not the only factor shaping phytoplankton

143 community structure in Sandusky Bay, since other shallow, turbid lakes are dominated by

144 *Microcystis* (e.g., Taihu Lake; Paerl et al., 2011) instead of *Planktothrix*. The ability to compete

145 for nutrients, or substrate affinity, likely plays an important role in distinguishing between

146 *Microcystis* blooms in western Lake Erie and *Planktothrix* blooms in Sandusky Bay. The goals

147 of this study were to: (1) quantify NH_4^+ regeneration and potential uptake dynamics and total

148 microbial community demand for NH_4^+ in Sandusky Bay during the summer bloom (June –

149 August); and (2) compare the kinetics of NH_4^+ uptake during a *Planktothrix*-dominated bloom in

150 Sandusky Bay and a *Microcystis*-dominated bloom in Maumee Bay. We hypothesized that NH_4^+

151 regeneration and potential uptake rates would increase through the summer as *in situ* DIN is

152 depleted and the *Planktothrix* bloom becomes more N stressed. Based on previous literature on

153 NH_4^+ uptake kinetics for *Microcystis* (Nicklisch and Khol 1983) and *Planktothrix* (Zevenboom

154 and Mur 1981), we hypothesized that the *Planktothrix*-dominated bloom in Sandusky Bay would

155 have higher affinity for NH_4^+, representing a competitive advantage at low NH_4^+ concentrations,

156 than the *Microcystis*-dominated bloom in Maumee Bay.

157
158
159 **2. Methods**
160 *2.1 Sample Collection*
161
162 Water samples from Sandusky Bay were collected on five occasions during summer

163 2017: June 5, June 26, July 31, August 14, and August 28. Surface water (top 20 cm) for NH_4^+

164 dynamics experiments was collected in 3 L Nalgene bottles and stored in a dark cooler until

165 processing. All experiments were commenced within three hours of sampling. Samples were

166 collected from four stations: Ohio Department of Natural Resources (ODNR) 4 and 6 in the inner

167 part of the bay, ODNR 2 in the outer bay, and Bells, located just outside the bay in Lake Erie

168 (Fig. 1). Samples for *in situ* nutrient analyses were filtered, with a 60 mL syringe, immediately in

169 the field using 0.2 µm Sterivex cartridge filters (Millipore) into 60 mL acid-washed polyethylene

170 bottles, stored in the dark on ice, and processed on the same day in the lab. Physico-chemical

171 parameters, including temperature and pH, were measured using a multi-parameter sonde (YSI

172 model 600 QS). Due to a malfunction in the dissolved oxygen (DO) probe on the YSI, daily DO

173 measurements, starting 28 June 2017, were generated using a Great Lakes Observing System

174 (GLOS) buoy located near ODNR 2 in Sandusky Bay. Water column DO values from June 5 and

175 26 were measured with a sonde deployed in the eastern outer bay (east of EC 1163; Fig. 1).

176 Turbidity was measured using Secchi depth as a proxy. Water for chlorophyll *a* Chl

177 *a* analysis was collected in amber bottles and stored on ice until return to the lab. Biomass

178 was collected on the same day onto 0.2 µm polycarbonate filters and stored at -20˚C until treated

179 with 10 mL of 90% acetone for 24 h. Chl *a* samples were analyzed with a Turner Designs

180   Fluorometer (TD-700) using manufacturer's standards (Welschmeyer, 1994). Ambient nutrient

181   analyses included NH_4^+, NO_2^-, NO_3^-, soluble reactive phosphorus (SRP), and total phosphorus

182   (TP) and was performed at the National Center for Water Quality Research (NCWQR) at

183   Heidelberg University.

184   Water samples for kinetic experiments in Maumee Bay were collected on three occasions

185   from site WE6 (July 17, August 14, and October 10), and once from site MB18 (August 9;

186   Fig.1), which is across the shipping channel from, and in close proximity to, WE6 (Fig. 1).

187   Sampling at WE6 occurred in conjunction with NOAA Great Lakes Environmental Research

188   Laboratory (GLERL) weekly sampling, whereas sampling at MB18 was conducted with Ohio

189   State University Stone Laboratory personnel. Surface water (top 1 m) was collected using a 5 L

190   Niskin bottle into a 10 L polyethylene cubitainer and stored in a dark cooler for transport to the

191   lab. Samples for nutrient analyses were immediately filtered in the field into 15 mL clear,

192   polypropylene tubes using 0.2 µm syringe filters (Nylon; Millipore), stored on ice in a dark

193   cooler, and then frozen at -20 ˚C until analysis. Nutrient analyses (NH_4^+, NO_2^-, NO_3^-, and

194   orthophosphate (OP)) were performed using a Lachat 8500 Quikchem nutrient analyzer (Hach).

195   Note that Sandusky Bay data, analyzed by the NCWQR at Heidelberg university, is reported as

196   SRP, whereas the Lachat used for Maumee Bay data measures OP. Chl *a* and geochemical data

197   (DO and temperature) from WE6 in Maumee Bay were accessed using the NOAA GLERL

198   annual data share and are single measurements for this station.

199
200   *2.2 NH$_4^+$ dynamics*

201   NH_4^+ uptake and regeneration experiments followed the protocol described in Hampel et

202   al., (2018). Briefly, 1 L of water from each station was amended with 98% $^{15}NH_4Cl$ (Isotec; final

203   concentration added 8–32 µM based on bloom status; i.e., higher concentrations during heavier

204 blooms to prevent total substrate depletion during incubation), mixed thoroughly, and decanted

205 into six 125 mL, clear Nalgene incubation bottles (three light incubations and three dark). Initial

206 samples were filtered through a 0.2 µm syringe filter, 12.5 mL into 15 mL clear, polypropylene

207 tubes (for total NH_4^+ analysis) and 12 mL with no headspace into Exetainers (for $^{15}NH_4^+$

208 analysis). Dark bottles were wrapped with aluminum foil and submerged with unwrapped light

209 bottles outside, submerged in water at near-ambient light and temperature for 18 h. After the

210 incubation period, final samples were collected as described for initial samples. Total ($^{14}N + {}^{15}N$)

211 NH_4^+ concentrations were analyzed using the Lachat nutrient analyzer. $^{15}NH_4^+$ concentrations

212 were measured using membrane inlet mass spectrometry (MIMS; Kana et al., 1994) combined

213 with oxidation to N_2 gas (OXMIMS; Yin et al. 2014). Samples for $^{15}NH_4^+$ analysis were treated

214 with 200 µl of hypobromite iodine solution (oxidizes $^{15}NH_4^+$ to $^{29/30}N_2$) and immediately

215 measured on the MIMS. $^{15}NH_4^+$ standards (from 0.1 to 100 µM) were analyzed at the beginning

216 and the end of each sample run. $^{15}NH_4^+$ concentrations were determined using the line equation

217 from the standard curve and total $^{15}N_2$ production ($^{29}N_2 + 2 * {}^{30}N_2$; Yin et al., 2014).

218   Potential NH_4^+ uptake rates and actual regeneration rates were calculated using the

219 Blackburn/Caperon isotope dilution model (Blackburn, 1979; Caperon et al., 1979; McCarthy et

220 al., 2013). In this model, potential uptake is calculated from the depletion of both $^{14}NH_4^+$ and

221 $^{15}NH_4^+$ pools, and regeneration is measured from dilution of the total NH_4^+ pool by regenerated

222 $^{14}NH_4^+$ and is considered an actual rate (Gardner et al., 2017).

223
224 *2.3 Community Biological Ammonium Demand (CBAD)*

225   CBAD is a conceptual model of internal NH_4^+ cycling proposed by Gardner et al. (2017).

226 CBAD is represented by the difference between measured potential NH_4^+ uptake rates and actual

227 regeneration rates during a bloom and reflects the net microbial community demand for NH_4^+.

228 Average values for CBAD in light and dark incubations were calculated as:

229 $$CBAD = ([NH_4^+]_0 - [NH_4^+]_t) / t$$

230 where $[NH_4^+]_0$ is total ($^{14}N+^{15}N$) NH_4^+ concentration at the initial time of incubation, $[NH_4^+]_t$ is

231 the total NH_4^+ concentration at the end of the incubation, and t is elapsed time in hours.

232 *2.4 Kinetic experiment*

233 The Michaelis–Menten model (Caperon and Meyer, 1972; Martens-Habbena et al., 2009)

234 was used to explore the kinetics of NH_4^+ uptake during *Planktothrix* and *Microcystis* blooms and

235 investigate the dependence of uptake rate on substrate concentrations. This model relates the

236 reaction rate and substrate concentration following the formula:

237 $$V_0 = (V_{max} [S]) / K_m + [S]$$
238
239 Where V_{max} is the maximum velocity of the reaction, S is the substrate concentration, and K_m is

240 the substrate concentration at $\frac{1}{2} V_{max}$.

241 To investigate the competitive abilities of different cyanobacteria in different parts of

242 Lake Erie, water from Sandusky Bay and Maumee Bay was collected as described above.

243 Unfiltered surface water collected in the field was transported to the lab and decanted into seven

244 125 mL, clear Nalgene bottles. One bottle was designated as a control and received no ^{15}N

245 additions. The remaining bottles were amended with increasing $^{15}NH_4^+$ concentrations ranging

246 from 0.25 µM to 16 µM at 5–6 substrate levels in Sandusky Bay and 4–5 in Maumee Bay. This

247 range of concentrations was chosen based on preliminary trials. The kinetic experiment followed

248 the protocol for NH_4^+ dynamics described above. Bottles were incubated at *in situ* temperature

249 and light for 5 h on June 5, June 26, July 17, July 31, August 28, and October 10, 2017. On

250 August 14, incubation time was limited to 15 min due to rapid NH_4^+ depletion. Uptake rates were

251 calculated as above and plotted against spike concentrations using Kaleidagraph software

252 (version 4.5.3) to create the Michaelis–Menten curve. Additionally, the Michaelis–Menten model

253 was run in RStudio (version 1.1.383) with the drm package (version 0.5-8) for combined

254 regression and association models.

255
256 *2.5 Metatranscriptomic analyses*
257
258 Biomass (500 mL) from several dates (June 8, June 22, July 6, July 13, August 3, and

259 August 31) during the summer 2015 bloom was collected in the field onto 0.2 µm Sterivex

260 cartridges, stored on dry ice, and placed in the -80 °C freezer until extractions. RNA was

261 extracted using the Mo Bio PowerWater Sterivex™ DNA Isolation Kit (now available as Qiagen

262 DNeasy® PowerWater® Sterivex™ Kit), with the alternate RNA Isolation protocol. Extracted

263 RNA (3-5 µg per sample) was stored at -80 °C until it was sent to HudsonAlpha Institute for

264 Biotechnology (Huntsville, AL) for RNA sequencing, where they were treated to reduce rRNA.

265 The reads were single-end reads of 50 base pairs. All samples were from outer Sandusky Bay

266 site ODNR 1, except for the June 8 sample taken at outer bay station EC 1163.

267 The metatranscriptome reads were trimmed, underwent quality control (QC) analysis, and

268 then were assembled using the CLC Workbench software version 9.5.3 (Qiagen). The CLC

269 Workbench 9.5.3 program removed failed sequences that did not pass QC according to the

270 default parameters. The remaining reads were assembled *de novo* into contigs, then mapped back

271 to assembled contigs using the reference genomes. Aligned RNA transcripts (RNAseq) files

272 were aligned to the following reference genomes: *Sulfurimonas denitrificans* DSM

273 1251, *Microcystis aeruginosa* NIES-843, *Desulfovibrio magneticus* RS-1, *Desulfovibrio*

274 *desulfuricans* ND132 (Final JGI assembly), *Anabaena cylindrica* PCC 7122, *Aphanizomenon*

275 *flos-aquae* NIES-81, *Klebsiella pneumoniae* 1158, and *Burkholderia pseudomallei* K96243. The

276 reference genomes were concatenated into a single reference library. An annotated genome of

277 *Planktothrix agardhii* from Sandusky Bay was obtained from Dr. Greg Dick at the University of

278 Michigan. These were selected to represent the different cyanobacteria and N fixers present in

279 metagenomic datasets obtained previously from Sandusky Bay.

280 The reference genomes were confirmed for the presence of *cphA, cphB, amt, glnA,* and

281 *nifH* genes by implementing a gene search on JGI IMG/M using the aforementioned sequences

282 plus *Planktothrix agardhii* NIVA CYA 126/8. The BLAST tool of the CLC Workbench program

283 was used to search for the gene sequence from each species of the reference genomes. Hits were

284 obtained with outputs of % identity, Greatest Hit Lengths, and E values for assessing relatedness

285 of the genes. Each of these sequences were then reconfirmed using the BLASTn and/or BLASTx

286 function using the NCBI database with the "dissimilar sequence" setting. The RNAseq files for

287 each date and site were filtered to find the corresponding Reads per Kilobase transcript per

288 Million mapped reads (RPKM) value for the gene in question.

289
290 *2.6 Statistical analysis*

291 All statistical analyses were performed using RStudio software (version 1.1.383).

292 Environmental data were checked for normality using the Shapiro–Wilk normality test.

293 Temperature and TP were the only normally distributed variables. To investigate potential

294 environmental drivers of NH_4^+ dynamics, a multivariate correlation analysis was performed

295 using the Spearman correlation method for nonparametric data. A *p*-value of < 0.05 was

296 considered statistically significant.

297

3. Results

298

3.1 Environmental variables in Sandusky and Maumee Bays

299

300   Water temperature in Sandusky Bay ranged from 20.4 °C to 24.5 °C (Table 1). DO

301   concentrations ranged from 9.18 to 9.71 mg L^{-1} between June and August 14 and decreased at

302   the end of August (8.67 mg L^{-1}). Chl a concentrations showed seasonal variability, with greatest

303   values at the end of June (mean = 75.2 ± 27.7 µg L^{-1}) and in July (mean = 122 ± 74.5 µg L^{-1}),

304   and lower concentrations in August (mean = 44.0 ± 21.4 µg L^{-1}; $p < 0.05$). Chl a concentrations

305   also varied spatially, with the Bells station in Lake Erie ranging from 5.80 to 44.8 µg L^{-1},

306   significantly lower than the ODNR stations (31.3 – 172 µg L^{-1}; $p < 0.05$). Lowest Chl a

307   concentrations at Bells corresponded with greatest Secchi depths at this station (80 – 132 cm). At

308   ODNR stations, within Sandusky Bay, Secchi depths were 32 – 43 cm throughout the summer

309   (not measured in July).

310   NH$_4^+$ concentrations in Sandusky Bay showed slight variation between June and August

311   14 (mean = 2.63 ± 0.49 µM; Table 1) but decreased significantly by August 28 (mean = 1.02 ±

312   0.32 µM; $p < 0.001$). NO$_2^-$ concentrations were below the detection limit at all times except July

313   31 at all stations and August 14 at Bells (Table 1). NO$_3^-$ concentrations gradually decreased from

314   62.0 – 251 µM at the beginning of June to 0 – 1.43 µM in August. SRP concentrations were

315   lowest in June (mean = 0.20 ± 0.09 µM) and greater in August (0.50 ± 0.20 µM; Table 1).

316   Water temperature in Maumee Bay decreased from 23.9 °C – 25.1 °C in August to 20.7

317   °C in October (Table 2). DO peaked in mid-August (9.59 mg L^{-1}) and was lower in July (5.87

318   mg L^{-1}) and October (5.72 mg L^{-1}). Chl a increased from June (3.5 µg L^{-1}) to August (532 µg L^{-1}

319   ) and decreased to 40.9 µg L^{-1} in October. Secchi depth was 50 cm in October and 20 cm in

320   August and June. Ambient NH$_4^+$ concentrations in Maumee Bay were highest in July (6.29 ±

321   0.03 μM) and decreased to undetectable by October. NO_2^- concentrations were highest in July

322   (5.13 ± 0.02 μM) and decreased to 0.02 ± 0.001 μM in October. A similar pattern was observed

323   for NO_3^- concentrations, with highest values in July (400 ± 0.9 μM) and lowest in October (0.40

324   ± 0.001 μM). OP was also highest in July (4.32 ± 0.04 μM) and decreased to 0.17 ± 0.01 μM in

325   October.

326
327   *3.2 Potential NH_4^+ uptake rates in Sandusky Bay*
328
329   Potential NH_4^+ uptake rates in light incubations ranged from 0.06 to 3.12 μmol L^{-1} h^{-1}

330   (Fig. 2A). Lower rates were consistently observed at Bells (mean = 0.16 ± 0.01 μmol L^{-1} h^{-1})

331   versus ODNR stations (mean = 1.78 ± 0.18 μmol L^{-1} h^{-1}; $p < 0.005$). Light uptake rates at ODNR

332   4, 6, and 2 were not different from each other ($p > 0.05$). At all stations, potential uptake rates in

333   light incubations increased through the summer bloom, with lowest rates in June (mean = $0.53 \pm$

334   0.08 μmol L^{-1} h^{-1}), higher rates in July (mean = 1.00 ± 0.07 μmol L^{-1} h^{-1}), and highest rates in

335   August (mean = 1.99 ± 0.20 μmol L^{-1} h^{-1}). However, differences were only significant between

336   June and August ($p < 0.05$). Light NH_4^+ uptake rates were positively correlated to ambient SRP

337   and TP concentrations and Chl *a* (Spearman $p < 0.005$) and negatively correlated to ambient

338   NO_3^- concentrations and Secchi depth (Spearman $p < 0.05$; Table 3).

339   Potential NH_4^+ uptake rates in dark incubations ranged from 0.02 to 3.00 μmol L^{-1} h^{-1}

340   (Fig. 2B). Lowest dark uptake rates were observed at Bells (mean = 0.09 ± 0.01 μmol L^{-1} h^{-1});

341   however, the statistical significance of this difference from the ODNR stations was marginal ($p =$

342   0.08). The three ODNR stations did not exhibit significant differences in dark uptake (mean =

343   1.22 ± 0.04 μmol L^{-1} h^{-1}; $p > 0.5$). Dark rates also increased throughout the summer, with lowest

344   rates in June (mean = 0.09 ± 0.01 μmol L^{-1} h^{-1}), higher rates in July (mean = 0.22 ± 0.01 μmol L^-

345   ^{1} h^{-1}), and highest rates in August (mean = 1.72 ± 0.06 μmol L^{-1} h^{-1}). Dark rates in August were

346 statistically different from those in June and July ($p < 0.05$). Dark uptake rates were positively

347 correlated to SRP and TP concentrations (Spearman $p < 0.05$) and negatively correlated to NO_3^-

348 concentration (Spearman $p < 0.05$; Table 3). Light and dark NH_4^+ uptake rates were statistically

349 different from each other only in July ($p = 0.05$), and neither were correlated to ambient NH_4^+

350 concentrations.

351
352 *3.3 Actual NH_4^+ regeneration rates in Sandusky Bay*

353   NH_4^+ regeneration rates in light and dark incubations were not statistically different, so

354 they were averaged together (Fig. 2C). Averaged NH_4^+ regeneration rates ranged from 0 to 1.54

355 $\mu mol\ L^{-1}\ h^{-1}$. Regeneration rates at Bells (mean = $0.05 \pm 0.01\ \mu mol\ L^{-1}\ h^{-1}$) were an order of

356 magnitude lower than at ONDR stations (mean = $0.75 \pm 0.10\ \mu mol\ L^{-1}\ h^{-1}$; $p < 0.05$). NH_4^+

357 regeneration rates increased from June (mean = $0.23 \pm 0.04\ \mu mol\ L^{-1}\ h^{-1}$) to July (mean = $0.34 \pm$

358 $0.04\ \mu mol\ L^{-1}\ h^{-1}$) and August ($0.87 \pm 0.12\ \mu mol\ L^{-1}\ h^{-1}$), and a statistical difference was

359 observed between June and August ($p = 0.05$). Regeneration rates were positively correlated to

360 TP and Chl *a* concentrations (Spearman $p < 0.05$) and negatively correlated to NO_3^-

361 concentration and Secchi depth (Spearman $p < 0.05$).

362

363 *3.4 CBAD*

364   CBAD followed a similar pattern as NH_4^+ uptake rates (Fig. 3A), increasing from June

365 (mean = $0.23 \pm 0.01\ \mu mol\ L^{-1}\ h^{-1}$) to August (mean = $1.07 \pm 0.03\ \mu mol\ L^{-1}\ h^{-1}$) across all

366 stations. Light CBAD values during the two sampling trips in August were twice as high as the

367 average of the other months (mean = $0.33 \pm 0.01\ \mu mol\ L^{-1}\ h^{-1}$).

368   Dark CBAD also increased over the summer (Fig. 3B), starting with negative values

369 (reflecting net NH_4^+ regeneration) in June. By the end of August, dark CBAD ($1.05 \pm 0.02\ \mu mol$

370   L^{-1} h^{-1}) was as high as light CBAD (1.12 ± 0.03 µmol L^{-1} h^{-1}). Light and dark CBAD were lowest

371   at Bells (0.10 ± 0.01 and 0.03 ± 0.01 µmol L^{-1} h^{-1}, respectively).

372

373   *3.5 NH_4^+ uptake kinetics*

374   K_m values in Sandusky Bay were highest in June (K_m = 8.7 µM; Fig. 4A) and ranged

375   from 1.4 to 1.8 µM in subsequent experiments. However, V_{max} increased from July to the end of

376   August (1.52 to 27.1 µmol L^{-1} h^{-1}, respectively).

377   K_m values in Maumee Bay showed the opposite pattern than observed in Sandusky Bay

378   (Fig. 4B). K_m values increased from July (K_m = 0.32 µM) to the highest value in October (K_m =

379   8.52 µM). However, V_{max} in Maumee Bay remained in a tight range from 0.20 to 0.53 µmol L^{-1}

380   h^{-1} for all experiments.

381
382   *3.6 Metatranscriptomic analysis of N metabolism*
383
384   During 2015, a series of Sandusky Bay metatranscriptomes obtained from June 8 to

385   August 31 examined *cphA, cphB, amt, glnA,* and *nifH* gene expression in *P. agardhii* during the

386   onset of N limitation (Fig. 5). *Planktothrix* expressed two distinct *cphA* genes, but at different

387   times in the season corresponding to N availability. *Planktothrix* has the *cphBA* operon and an

388   independent *cphA* (Forchhammer and Bjorn, 2016). The independent *cphA* (*cphA1*) was

389   expressed when N was replete. *cphA2* was expressed, along with *cphB*, when N levels were low.

390   No *Microcystis cphA* expressions were detected.

391   In early summer, when NH_4^+ and NO_3^- concentrations were high (Fig. 5A, B) due to

392   riverine discharge following spring rains (Salk et al., 2018), *cphA1* was highly transcribed,

393   suggesting luxury N storage via cyanophycin synthesis (Gupta and Carr 1981; Allen 1984;

394   Forchhammer and Bjorn 2016). When NH_4^+ and NO_3^- were depleted in late summer, no *cphA1*

395   expression was detected, and *cphBA2* operon transcription was activated (Fig. 5A), suggesting

396   cyanophycin degradation (Richter et al., 1999; Ponndorf et al., 2017) as an adaptation to N

397   limitation. Reflecting the increased competition for N was the expression of *glnA* in late summer,

398   encoding glutamine synthetase, the high affinity assimilation pathway for NH_4^+ (Reyes et al.,

399   1997). Genes for NH_4^+ transporters *amt1* and *amt3* were transcribed constitutively throughout

400   the summer (Fig. 5B).

401   Earlier work documented the presence of a minor community of N-fixing cyanobacteria

402   during the *Planktothrix*-dominated bloom (Salk et al. 2018). 16S rRNA reads assigned to

403   *Nostocales* (predominantly *Aphanizomenon* spp. and *Dolichospermum* spp.) reached up to 25%

404   of total cyanobacterial reads on a few occasions in 2015 before complete N depletion (Fig. 5B),

405   but *Nostocales* reads were usually very low.

406
407
408   **4. Discussion**
409
410   *4.1 Potential NH_4^+ uptake and CBAD*
411
412   Nutrient concentrations and NH_4^+ dynamics exhibited expected patterns during the 2017

413   *Planktothrix* bloom in Sandusky Bay. After bloom initiation, DIN concentrations in the bay

414   decreased to low or undetectable levels (Table 1), with NO_3^- often below detection, and

415   detectable but low NH_4^+ concentrations. This pattern is consistent with previous work in

416   Sandusky Bay (Chaffin et al., 2018; Salk et al., 2018) and suggests a high demand and

417   competition for N in late summer. NH_4^+ uptake rates in light incubations increased throughout

418   the summer at all stations, with late August rates approximately four times higher than those in

419   June in the bay (ODNR 2, 4, and 6) and five times greater outside of the bay at Bells (Fig. 2A).

420   As expected, these light uptake rates were correlated positively with Chl *a* ($p < 0.005$; Table 3),

421   suggesting an increase in photoautotrophic activity. At Bells, where Chl *a* was consistently

422   below bloom thresholds (< 20 µg L^{-1}; Xu et al., 2015), NH$_4^+$ uptake rates (and CBAD) were

423   predictably lower than those at sites within Sandusky Bay. The NH$_4^+$ uptake rates reported in this

424   study for Sandusky Bay are consistent with those reported in other freshwater, eutrophic,

425   cyanoHAB-impacted lakes (Gu et al., 1997; Présing et al., 2001; James et al., 2011; McCarthy et

426   al., 2013; Hampel et al., 2018).

427   Light uptake rates reported in this study are an order of magnitude greater that those

428   reported recently in Sandusky Bay (Salk et al., 2018). In comparison with similarly eutrophic

429   systems, those rates were exceptionally low, indeed more comparable to those measured in

430   oligotrophic lakes (e.g., Suttle and Harrison 1988), including Lake Michigan in late winter and

431   spring (Gardner et al., 2004). Stable isotope additions used in Salk et al., (2018) were tracer-level

432   (i.e., <10 % of the ambient DIN pool) and may have underestimated NH$_4^+$ cycling rates due to

433   complete substrate depletion before incubations were ended (Paasche 1988). Substrate depletion

434   is especially problematic in highly productive systems, like Sandusky Bay; thus, we applied

435   saturating-level stable isotope amendments, which are better suited for highly dynamic,

436   eutrophic systems with high cyanobacterial biomass. Saturating additions of substrate can alter

437   steady-state conditions (Glibert et al., 1988); therefore, NH$_4^+$ uptake rates reported in this study

438   are qualified as potential rates, but results from saturating- and tracer-level isotope amendments

439   tend to converge in eutrophic systems with high ambient NH$_4^+$ concentrations (Glibert et al.,

440   1982).

441   Dark NH$_4^+$ uptake rates also increased with time at the bay stations and, to a lesser extent,

442   at Bells (Fig. 2B). By late August, dark NH$_4^+$ uptake rates were not distinguishable from light

443   uptake rates. Dark uptake rates in Sandusky Bay were higher than those observed in other

444   eutrophic lakes affected by cyanoHABs (James et al., 2011; McCarthy et al., 2013; Hampel et

445   al., 2018), suggesting an important role for heterotrophic organisms. Some photoautotrophs can

446   assimilate NH_4^+ in the dark under N limiting conditions (e.g., Cochlan et al., 1991); however, our

447   saturating-level $^{15}NH_4^+$ additions likely minimized this effect. Dark uptake rates were not

448   correlated with Chl a concentration (Table 3); thus, when NH_4^+ is scarce and competition for

449   NH_4^+ is extreme in late summer, heterotrophic partnerships with cyanobacteria in the

450   phycosphere may become important (Steffen et al., 2012).

451   The phycosphere concept was introduced by Bell and Mitchel (1972) and is analogous to

452   the rhizosphere concept in soils. In mixed microbial assemblages, heterotrophic bacteria can

453   simultaneously regenerate and assimilate NH_4^+ (Tupas and Koike, 1991). These bidirectional

454   interactions have been studied in diatoms, dinoflagellates, and other cyanobacteria (Amin et al.,

455   2015; Lupette et al., 2016), yet little is known about phycosphere interactions during

456   cyanobacterial blooms. Phycosphere interactions might play a key role in dynamic, eutrophic

457   ecosystems, where competition for nutrients is high, and microbial interactions in the water

458   column are complex. For example, NH_4^+ uptake by heterotrophic bacteria has been previously

459   studied, mostly in marine environments (Kirchman et al., 1990; Tupas and Koike, 1991).

460   Heterotrophic uptake of NH_4^+ in the light has been shown to increase with decreasing ambient

461   concentrations (Kirchman et al., 1990), suggesting that heterotrophic bacteria can outcompete

462   phytoplankton at low NH_4^+ concentrations. Our NH_4^+ cycling patterns support these findings and

463   suggest that Sandusky Bay exhibits similarly complex microbial interactions between

464   cyanobacteria and heterotrophic partners.

465   The CBAD model represents NH_4^+ dynamics and microbial productivity in N depleted

466   systems (Gardner et al., 2017), and thus is a useful metric to investigate NH_4^+ cycling in

467   Sandusky Bay. CBAD reflects the demand of the entire microbial community, including (light

468   CBAD) and excluding photoautotrophs (dark CBAD; Gardner et al., 2017), assuming that

469   photoautotrophs were not active in dark incubations. Within the bay, light CBAD followed the

470   pattern of light uptake rates, with the largest increase observed between July 31 and August 14.

471   Dark CBAD was negative, reflecting net NH_4^+ regeneration by the microbial community, or low

472   in June and July (Fig. 3), indicating that demand for NH_4^+ in the dark was largely met by the

473   supply from regeneration (Gardner et al., 2017). However, dark CBAD was not distinguishable

474   from light CBAD in August, concomitant with decreased chlorophyll, suggesting that the

475   increased dark CBAD reflects increased demand by non-photoautotrophs.

476   *4.2 NH_4^+ Regeneration*

477   NH_4^+ regeneration rates at ODNR 6, 4, and 2 followed the same general pattern as uptake

478   rates, with lowest values in June and highest in August. At these stations, regeneration rates at

479   the end of August were almost twice as high as those in June, suggesting that N depletion by the

480   bloom caused photoautotrophs to rely on regenerated NH_4^+ from increased heterotrophic activity

481   and bloom biomass remineralization to support growth. While regeneration can supply

482   substantial amount of NH_4^+, high biomass creates a great demand for N in August. The

483   proportion of uptake supported by regeneration increased throughout the summer (Fig. 2C). In

484   outer Sandusky Bay (ODNR 2), regeneration could support 36 – 40% of potential light NH_4^+

485   uptake. This proportion increased to 50% by the end of August, a pattern that is magnified in

486   potential importance considering the large increase in uptake rates from June to August.

487   Increasing dependence on regeneration corresponded with low ambient N concentrations in the

488   bay, further highlighting the important role of recycled NH_4^+ in supporting cyanoHAB growth

489   and bloom maintenance. Other cyanoHAB-impacted lakes exhibit similar patterns of

490   dependence on NH_4^+ regenerated in the water column, including Lake Taihu (Paerl et al. 2011;

491   Hampel et al., 2018), Lake Balaton (Présing et al., 2001), Lake Biwa (Haga et al., 1995;

492   Takahashi et al., 1995), and Missisquoi Bay, Lake Champlain (McCarthy et al. 2013).

493   To compare regenerated NH_4^+ rates in the water column to external N loading, we

494   extrapolated average NH_4^+ regeneration rates from ODNR 6, 4, and 2 to the whole-bay volume

495   (0.423 km^3; Conroy et al., 2007). Daily Sandusky River flow data and total N (TN) and total

496   Kjeldahl N (TKN; $TN = TKN + NO_3^- + NO_2^-$) concentrations from 2017 were obtained from the

497   NCWQR (https://ncwqr.org) and used to calculate daily and annual external N loading. Annual

498   TN loading from the Sandusky River (October 2016 – September 2017; the NCWQR database

499   was not updated beyond September 2017 as of manuscript preparation) introduced 8.58×10^3

500   metric tons of N into the bay during this 12 month period. Average summer regeneration from

501   our incubations (June–August 2017) recycled 6.6×10^3 metric tons of N as NH_4^+. In just the

502   three summer months evaluated, regeneration in the water column provided bioavailable N for

503   primary production at the level equivalent to ~$77 \pm 7\%$ of the annual N load.

504   When extrapolated to the whole bay volume, daily NH_4^+ regeneration exceeded daily TN

505   loading at all sampling events (Table 4). During the week of June 5, regeneration contributed 2–

506   5 times more N than the Sandusky River. During the week of July 31, regeneration provided 25–

507   53 times more N than the river and, by the end of August, over 1000 times more N than the river

508   (Table 4). While the contribution of regeneration increased throughout the summer, TN and

509   TKN loading from the river decreased along with discharge. However, the proportion of TKN to

510   TN in Sandusky River loading increased from 13.2 % at the beginning of June to 91.9% by the

511   end of August (Table 4), highlighting the importance of considering N forms and potential

512   bioavailability in external loading.

513   This exercise exemplifies the critical role of internally recycled NH_4^+ during summer in

514   sustaining the *Planktothrix* bloom, especially when ambient N was depleted. The large mass of

515   internally recycled NH_4^+, driven by high external N loads from the watershed, is critical

516   information for resource managers and regulators, who often base management decisions on

517   ecosystem models that do not sufficiently consider the effects of internal N dynamics on

518   eutrophication issues. Monitoring nutrient concentrations in eutrophic systems, while valuable,

519   does not provide a sufficient characterization of these nutrient dynamics. High microbial demand

520   and turnover rates can cause highly bioavailable nutrients, such as NH_4^+, to be undetectable or

521   measured at low concentrations, even though their recycling rates are largely supporting system

522   productivity at critical times (McCarthy et al., 2013).

523   *4.3 NH_4^+ uptake kinetics*

524   Kinetic NH_4^+ uptake experiments in Sandusky and Maumee Bays exhibited opposite

525   patterns, suggesting that these microbial communities were distinctive (Fig. 4). K_m is often used

526   to represent the affinity of a microbe for a substrate. Microbes with a low K_m have a competitive

527   advantage at low nutrient concentrations and are excellent scavengers (Martens-Habbena et al.,

528   2009). However, microbes with a high K_m thrive at high substrate concentrations and can

529   assimilate more substrate before reaching saturation. With different K_m values, microbes can fill

530   different niches in the environment to maximize their competitive abilities.

531   In Sandusky Bay (*Planktothrix*-dominated community; Davis et al., 2015; Salk et al.,

532   2018), the highest K_m was observed in June, and it then decreased and stabilized throughout July

533   and August. While K_m remained relatively constant in July and August, we observed a dramatic,

534   significant increase in V_{max} from the end of July ($V_{max} = 1.52$ µmol $L^{-1} h^{-1}$) through August (V_{max}

535     $= 27.1$ µmol $L^{-1} h^{-1}$), which reflects strong competition for depleted NH_4^+. The increase in V_{max}

536　corresponded to significant increases in dark NH_4^+ uptake rates between the end of July and

537　through August (Fig. 2). When NH_4^+ availability in the water column is low, dead and dying

538　cells may be rapidly remineralized in the phycosphere, which may help explain increased

539　heterotrophic activity (e.g., Gardner and Lee 1975). The constant and relatively low K_m of the

540　late summer, *Planktothrix*–dominated community illustrates the strong affinity for NH_4^+ during

541　N limited conditions. K_m values reported for NH_4^+ in *Planktothrix* are lacking both in culture and

542　natural environments. One study investigated NH_4^+ uptake kinetics in chemostats under NO_3^-

543　limitation and reported K_m values of 8 ± 3 µM (Zevenboom and Mur, 1981), which are

544　comparable to our values from June, but higher than those from late summer.

545　　　　In contrast, K_m values in Maumee Bay increased from July (0.32 µM) to August (3.53

546　µM) and October (8.52 µM). This pattern may reflect the rapid increase in *Microcystis*-

547　dominated cyanoHABs in Maumee Bay commonly observed in August and lasting into October

548　(Steffen et al., 2014). Unlike Sandusky Bay, V_{max} in Maumee Bay was consistent (0.20–0.53

549　µmol $L^{-1} h^{-1}$), perhaps suggesting that competition for NH_4^+ in Maumee Bay was less intense than

550　in Sandusky Bay. The Maumee River watershed (21,540 km^2) is 4.5 times larger than the

551　Sandusky River watershed (4,727 km^2), and, accordingly, the Maumee River supplied 66.8

552　metric tons of TN to western Lake Erie in August 2017, while the Sandusky River supplied 13.2

553　metric tons of TN to Sandusky Bay (NCWQR). DIN concentrations in 2017 were very low in

554　Sandusky Bay from August through late summer (Table 1), but DIN concentrations were still

555　high (> 100 µM, mostly comprised of NO_3^-) in Maumee Bay in August (Table 2). Thus, while

556　DIN in Sandusky Bay was scarce, *Microcystis* was not as substrate limited, perhaps affecting

557　measured K_m and V_{max} values. Additionally, light and dark NH_4^+ uptake (0.125 and 0.058 µmol

558　$L^{-1} h^{-1}$, respectively) and regeneration rates (0.162 µmol $L^{-1} h^{-1}$) at MB18 in August were 10–20

559   times lower than those in Sandusky Bay (Hampel et al., unpublished data). These results support

560   the hypothesis that substrate competition was not as extreme in Maumee Bay as in Sandusky

561   Bay.

562   The reported range of *Microcystis* K_m values is broad, including values up to 37 µM in

563   culture (Niklish and Khol 1983) and 113 µM in hypereutrophic Lake Taihu (Yang et al., 2017).

564   Thus, *Microcystis* can assimilate substantial amounts of NH_4^+ before becoming saturated.

565   Overall, the results of this kinetic comparison suggest that, during the peak of a summer bloom

566   when NH_4^+ was depleted, *Planktothrix* had a competitive advantage in its high affinity for NH_4^+,

567   while N conditions in larger Maumee Bay allowed for less competition for substrate in the

568   *Microcystis*-dominated community.

569
570   *4.4 Metatranscriptome*
571
572   The transcriptional data in this paper address gene expression for N assimilation and

573   storage functions within an active bloom. The data differ from what is observed in pure cultures

574   of model cyanobacteria. Studies with *Dolichospermum (Anabaena)* and *Synechocystis* reveal

575   cyanophycin synthesis during decreases in N, and amendment of N-starved cyanobacteria with

576   exogenous NH_4^+ resulted in accumulation of cyanophycin (Mackerras et al., 1990). Cyanophycin

577   is also responsive to shifts in light and nutrients (Allen, 1984; Van de Waal et al., 2010). It is

578   unclear how these other factors may influence *cphA1* and *cphBA2* expression, but the pattern

579   observed in Sandusky Bay suggests that cyanophycin synthesis and degradation is a strategy for

580   *Planktothrix* success in a system prone to strong shifts in N availability. The expression of *glnA*,

581   under the control of *ntcA*, a transcriptional activator and sensor of intracellular C:N ratios (Zhao

582   et al., 2010), is also consistent with the observed declines in N concentrations. The *amt*

583   expression is present across the sampling season and consistent with N supply from regeneration.

584   Patterns of N depletion in the summer and sustained *Planktothrix* blooms are well-

585   documented in Sandusky Bay (Davis et al., 2015; Chaffin et al., 2018; Salk et al., 2018). The

586   community composition in the present study resembled that of all prior years sampled:

587   *Planktothri*x-dominated, with a minor fraction (5–20% of 16S rRNA reads) of N fixing

588   cyanobacteria (Salk et al., 2018). While the field study described here was completed in 2017,

589   metatranscriptomic data from 2015 can help elucidate genetic mechanisms for physiological

590   processes underlying *Planktothrix* success in an N limited system. Early in the summer, when

591   ambient bioavailable N concentrations were greater, genes for synthesis of the N-rich compound

592   cyanophycin were transcribed, suggesting luxury uptake and N storage, as demonstrated in

593   laboratory studies (Van de Waal et al., 2010). As ambient N was depleted late in the summer, the

594   cyanophycinase gene was transcribed, mobilizing stored N from an intracellular pool to help

595   meet metabolic N requirements. Concurrently, *glnA,* transcribed following N depletion, and

596   constitutive *amt* transcription reveal active mechanisms to acquire extracellular NH_4^+. Together,

597   these mechanisms of luxury uptake during N replete conditions, and high affinity NH_4^+ transport

598   throughout the bloom, contribute to *Planktothrix* dominance as N is depleted in summer.

599   Despite the dominance of *Planktothrix* in Sandusky Bay for most of the bloom season,

600   both cyanobacterial N-fixation (Salk et al., 2018) and *nif* transcription were detected as N

601   concentrations decreased, supporting the interpretation from NH_4^+ dynamics and transcriptomic

602   results that the cyanobacterial community evolved to N limitation over the course of the bloom

603   season.

604
605   **5. Conclusions**
606
607   The results presented in this study highlight the dynamic nature of eutrophic Sandusky

608   Bay during the *Planktothrix* bloom. Specifically, we emphasize the importance of internal NH_4^+

609   regeneration in sustaining summer non-N_2 fixing CyanoHABs, and likely influencing their

610   toxicity as well (Davis et al., 2015). Internal NH_4^+ cycling and rapid NH_4^+ turnover rates should

611   be considered in ecosystem models used to inform nutrient management strategies, which should

612   incorporate dual nutrient management (N and P) efforts to prevent and mitigate non-N_2 fixing

613   cyanoHABs in eutrophic lakes. Monitoring NH_4^+ turnover rates, rather than focusing solely on

614   ambient nutrient monitoring, can improve our understanding of the aquatic N cycle in eutrophic

615   lakes affected by cyanoHABs and how regeneration contributes to sustaining cyanoHABs.

616
617

629
630
631
632

References:

Allen, M. M., 1984. Cyanobacterial cell inclusions. Annu. Rev. Microbiol. 38, 1–25.

Amin, S.A., Hmelo, L.R., van Tol, H.M., Durham, B.P., Carlson, L.T., Heal, K.R., Morales, R.L., Berthiaume, C.T., Parker, M.S., Djunaedi, B., Ingalls, A.E., Parsek, M.R., Moran, M.A., Armbrust, E. V., 2015. Interaction and signalling between a cosmopolitan phytoplankton and associated bacteria. Nature 522, 98–101.

An, S., Joye, S.B., 2001. Enhancement of coupled nitrification-denitrification by benthic photosynthesis in shallow estuarine sediments. Limnol. Oceanogr. 46, 62–74.

Bell, W., Mitchell, R., 1972. Chemotactic and growth responses of marine bacteria to algal extracellular products. The Biological Bulletin 143, 265–277.

Blackburn, T.H., 1979. Method for Measuring Rates of NH(4) Turnover in Anoxic Marine Sediments, Using a N-NH(4) Dilution Technique. Appl. Environ. Microbiol. 37, 760–765.

Blomqvist, P., Pettersson, A., Hyenstrand, P., 1994. Ammonium-nitrogen: A key regulatory factor causing dominance of non-nitrogen-fixing cyanobacteria in aquatic systems. Arch. Hydrobiol. 132, 141–164.

Caperon, J., Meyer, J., 1972. Nitrogen-limited growth of marine phytoplankton—2. Uptake kinetics and their role in nutrient limited growth of phytoplankton. Deep-Sea Res. 19, 619–632.

Caperon, J., Schell, D., Hirota, J., Laws, E., 1979. Ammonium excretion rates in Kaneohe Bay, Hawaii, measured by a 15N isotope dilution technique. Mar. Biol. 54, 33–40.

Chaffin, J.D., Bridgeman, T.B., 2014. Organic and inorganic nitrogen utilization by nitrogen-stressed cyanobacteria during bloom conditions. J. Appl. Phycol. 26, 299–309.

Chaffin, J.D., Davis, T.W., Smith, D.J., Baer, M.M., Dick, G.J., 2018. Interactions between nitrogen form, loading rate, and light intensity on Microcystis and Planktothrix growth and microcystin production. Harmful Algae 73, 84–97.

Cochlan, W.P., Harrison, P.J., Denman, K.L., 1991. Diel periodicity of nitrogen uptake by marine phytoplankton in nitrate- rich environments. Limnol. Oceanogr. 36, 1689–1700.

Conroy, J.D., Quinlan, E.L., Kane, D.D., Culver, D.A., 2007. Cylindrospermopsis in Lake Erie: Testing its Association with Other Cyanobacterial Genera and Major Limnological Parameters. J. Gt. Lakes Res. 33, 519–535.

Davis, T.W., Bullerjahn, G.S., Tuttle, T., McKay, R.M., Watson, S.B., 2015. Effects of Increasing Nitrogen and Phosphorus Concentrations on Phytoplankton Community Growth and Toxicity during Planktothrix Blooms in Sandusky Bay, Lake Erie. Environ. Sci. Technol. 49, 7197–7207.

Forchhammer, K., Björn W., 2016. Closing a gap in cyanophycin metabolism. Microbiology 162, 727–729.

Gardner, W.S., Lee, G.F., 1975. The role of amino acids in the nitrogen cycle of Lake Mendota. Limnol. Oceanogr. 20, 379–388.

Gardner, W. S., Lavrentyev, P. J., Cavaletto, J. F., McCarthy, M. J., Eadie, B. J., Johengen, T. H., Cotner, J. B., 2004. Distribution and dynamics of nitrogen and microbial plankton in southern Lake Michigan during spring transition 1999-2000. J. Geophys. Res. 109

Gardner, W.S., Newell, S.E., McCarthy, M.J., Hoffman, D.K., Lu, K., Lavrentyev, P.J., Hellweger, F.L., Wilhelm, S.W., Liu, Z., Bruesewitz, D.A., Paerl, H.W., 2017. Community Biological Ammonium Demand: A Conceptual Model for Cyanobacteria Blooms in Eutrophic Lakes. Environ. Sci. Technol. 51, 7785–7793.

679 Glibert, P. M., 1988. Primary productivity and pelagic nitrogen cycling. In:
680   Blackburn, T. H., and Sorensen, J. (eds.), Nitrogen Cycling in Coastal Marine
681   Environments. John Wiley & Sons, Chichester. pp 3–31.
682 Glibert, P.M., Wilkerson, F.P., Dugdale, R.C., Raven, J.A., Dupont, C.L., Leavitt, P.R., Parker,
683   A.E., Burkholder, J.M., Kana, T.M., 2016. Pluses and minuses of ammonium and nitrate
684   uptake and assimilation by phytoplankton and implications for productivity and community
685   composition, with emphasis on nitrogen-enriched conditions. Limnol. Oceanogr. 61, 165–
686   197.
687 Gobler, C.J., Burkholder, J.M., Davis, T.W., Harke, M.J., Johengen, T., Stow, C.A., Van de
688   Waal, D.B., 2016. The dual role of nitrogen supply in controlling the growth and toxicity of
689   cyanobacterial blooms. Harmful Algae 54, 87–97.
690 Gu, B., Havens, K.E., Schelske, C.L., Rosen, B.H., 1997. Uptake of dissolved nitrogen by
691   phytoplankton in a eutrophic subtropical lake. J. Plank. Res. 19, 759–770.
692 Gupta, M., Carr, N.G., 1981. Enzyme activities related to cyanophycin metabolism in heterocysts
693   and vegetative cells of Anabaena spp. Microbiology 125, 17–23.
694 Haga, H., Nagata, T., Sakamoto, M., 1995. Size-fractionated NH4+ regeneration in the pelagic
695   environments of two mesotrophic lakes. Limnol. Oceanogr. 40, 1091–1099.
696 Hampel, J.J., McCarthy, M.J., Gardner, W.S., Zhang, L., Xu, H., Zhu, G., Newell, S.E., 2018.
697   Nitrification and ammonium dynamics in Taihu Lake, China: seasonal competition for
698   ammonium between nitrifiers and cyanobacteria. Biogeosciences 15, 733–748.
699 Havens, K.E., Fukushima, T., Xie, P., Iwakuma, T., James, R.T., Takamura, N., Hanazato, T.,
700   Yamamoto, T., 2001. Nutrient dynamics and the eutrophication of shallow lakes
701   Kasumigaura (Japan), Donghu (PR China), and Okeechobee (USA). Environ. Pollut. 111,
702   263–272.
703 James, R.T., Gardner, W.S., McCarthy, M.J., Carini, S.A., 2011. Nitrogen dynamics in Lake
704   Okeechobee: Forms, functions, and changes. Hydrobiologia 669, 199–212.
705 Kana, T.M., Darkangelo, C., Hunt, M.D., Oldham, J.B., Bennett, G.E. and Cornwell, J.C., 1994.
706   Membrane inlet mass spectrometer for rapid high-precision determination of N2, O2, and
707   Ar in environmental water samples. Anal. Chem. 66, 4166–4170.
708 Kirchman, D.L., Keil, R.G., Wheeler, P.A., 1990. Carbon limitation of ammonium uptake by
709   heterotrophic bacteria in the subarctic Pacific. Limnol. Oceanogr. 35, 1258–1266.
710 Kurmayer, R., Blom, J.F., Deng, L., Pernthaler, J., 2015. Integrating phylogeny , geographic
711   niche partitioning and secondary metabolite synthesis in bloom-forming Planktothrix. ISME
712   J. 9, 909–921.
713 Lupette, J., Lami, R., Krasovec, M., Grimsley, N., Moreau, H., Piganeau, G., Sanchez-Ferandin,
714   S., 2016. Marinobacter dominates the bacterial community of the Ostreococcus Tauri
715   phycosphere in culture. Front. Microbiol. 7, 1–14.
716 Mackerras, A.H., de Chazal, N.M., Smith, G.D., 1990. Transient accumulations of cyanophycin
717   in Anabaena cylindrica and Synechocystis 6308. Microbiology 136, 2057–2065.
718 Martens-Habbena, W., Berube, P.M., Urakawa, H., De La Torre, J.R., Stahl, D.A., Torre, J.,
719   2009. Ammonia oxidation kinetics determine niche separation of nitrifying Archaea and
720   Bacteria. Nature 461, 976–979.
721 McCarthy, M.J., Gardner, W.S., Lehmann, M.F., Bird, D.F., 2013. Implications of water column
722   ammonium uptake and regeneration for the nitrogen budget in temperate, eutrophic
723   Missisquoi Bay, Lake Champlain (Canada/USA). Hydrobiologia 718, 173–188.
724 McCarthy, M.J., James, R.T., Chen, Y., East, T.L., Gardner, W.S., 2009. Nutrient ratios and

725   phytoplankton community structure in the large, shallow, eutrophic, subtropical Lakes
726   Okeechobee (Florida, USA) and Taihu (China). Limnology 10, 215–227.

727 Millie, D.F., Fahnenstiel, G.L., Bressie, J.D., Pigg, R.J., Rediske, R.R., Klarer, D.M., Tester,
728   P.A., Litaker, R.W., 2009. Late-summer phytoplankton in western Lake Erie (Laurentian
729   Great Lakes): bloom distributions, toxicity, and environmental influences. Aquat. Ecol. 43,
730   915–934.

731 Nicklisch, A., Kohl, J.G., 1983. Growth kinetics of Microcystis aeruginosa (Kütz) Kütz as a
732   basis for modelling its population dynamics, Internationale Revue der gesamten
733   Hydrobiologie und Hydrographie 68, 317–326.

734 Oberhaus, L., Briand, J.F., Leboulanger, C., Jacquet, S., Humbert, J.F., 2007. Comparative
735   effects of the quality and quantity of light and temperature on the growth of Planktothrix
736   agardhii and P. rubescens. J. Phycol. 43, 1191–1199.

737 Paasche, E. 1988. Pelagic primary production in nearshore waters. In: Blackburn, T. H.
738   and Sorensen, J. (eds.), Nitrogen Cycling in Coastal Marine Environments. John Wiley &
739   Sons, Chichester, 33–57

740 Paerl, H.W., Xu, H., McCarthy, M.J., Zhu, G., Qin, B., Li, Y., Gardner, W.S., 2011. Controlling
741   harmful cyanobacterial blooms in a hyper-eutrophic lake (Lake Taihu, China): The need for
742   a dual nutrient (N & P) management strategy. Water Res. 45, 1973–1983.

743 Présing, M., Herodek, S., Preston, T., Vörös, L., 2001. Nitrogen uptake and the importance of
744   internal nitrogen loading in Lake Balaton. Freshwater Biol. 46, 125–139.

745 Ponndorf, D., Ehmke, S., Walliser, B., Thoss, K., Unger, C., Görs, S., Daş, G., Metges, C.C.,
746   Broer, I., Nausch, H., 2017. Stable production of cyanophycinase in Nicotiana benthamiana
747   and its functionality to hydrolyse cyanophycin in the murine intestine. Plant Biotechnol.
748   J, 15, 605–613.

749 Reyes, J.C., Muro-Pastor, M.I., Florencio, F.J., 1997. Transcription of glutamine synthetase
750   genes (glnA and glnN) from the cyanobacterium Synechocystis sp. strain PCC 6803 is
751   differently regulated in response to nitrogen availability. J. Bacteriol. 179, 2678–2689.

752 Richards, R.P., Baker, D.B., Crumrine, J.P., Stearns, A.M., Erie, L., 2010. Unusually large loads
753   in 2007 from the Maumee and Sandusky Rivers, tributaries to Lake Erie. J. Soil Water
754   Conserv. 65, 450–462.

755 Richter, R., Hejazi, M., Kraft, R., Ziegler, K., Lockau, W., 1999. Cyanophycinase, a peptidase
756   degrading the cyanobacterial reserve material multi-L-arginyl-poly-L-aspartic acid
757   (cyanophycin). FEBS J. 263, 163–169.

758 Rinta-Kanto, J.M., Wilhelm, S.W., 2006. Diversity of microcystin-producing cyanobacteria in
759   spatially isolated regions of Lake Erie. Appl. Environ. Microbiol. 72, 5083–5085.

760 Rücker, J., Wiedner, C., Zippel, P., 1997. Factors controlling the dominance of Planktothrix
761   agardhii and Limnothrix redekei in eutrophic shallow lakes. Hydrobiologia, 342, 107–115.

762 Scheffer, M., Rinaldi, S., Gragnani, A., Mur, L.R., van Nes, E.H., 1997. On the dominance of
763   filamentous cyanobacteria in shallow, turbid lakes. Ecology 78, 272–282.

764 Salk, K.R., Bullerjahn, G.S., Mckay, R.M.L., Chaffin, J.D., Nathaniel, E., 2018. Nitrogen
765   cycling in Sandusky Bay, Lake Erie: oscillations between strong and weak export and
766   implications for harmful algal blooms. Biogeosciences 15, 2891–2907.

767 Scheffer, M., Rinaldi, S., Mur, L.R., 1994. On the dominance of filamentous blue-green algae in
768   shallow lakes. Iiasa 78, 272–282.

769 Steffen, M.M., Li, Z., Effler, T.C., Hauser, L.J., Boyer, G.L., Wilhelm, S.W., 2012. Comparative
770   metagenomics of toxic freshwater cyanobacteria bloom communities on two

771   continents. PloS one 7, e44002.
772   Steffen, M.M., Belisle, B.S., Watson, S.B., Boyer, G.L., Wilhelm, S.W., 2014. Status, causes and
773   controls of cyanobacterial blooms in Lake Erie. J. Gt. Lakes Res. 40, 215–225.
774   Steffen, M.M., Belisle, B.S., Watson, S.B., Boyer, G.L., Bourbonniere, R.A., Wilhelm, S.W.,
775   2015. Metatranscriptomic evidence for co-occurring top-down and bottom-up controls on
776   toxic cyanobacterial communities. Appl. Environ. Microbiol. 81, 3268–3276.
777   Suda, S., Watanabe, M.M., Otsuka, S., Mahakahant, A., Yongmanitchai, W., Nopartnaraporn,
778   N., Liu, Y., Day, J.G., 2002. Taxonomic revision of water-bloom-forming species of
779   oscillatorioid cyanobacteria. Int. J. Syst. Evol. Microbiol. 52, 1577–1595.
780   Suttle, C.A., Harrison, P.J., 1988. Ammonium and phosphate uptake rates, N: P supply ratios,
781   and evidence for N and P limitation in some oligotrophic lakes. Limnol. Oceanogr. 33, 186–
782   202.
783   Takahashi, M., Hama, T., Matsunaga, K., Handa, N., 1995. Nitrogenous nutrient uptake by
784   phytoplankton and ammonium regeneration by microbial assemblage in Lake Biwa. J.
785   Plank. Res. 17, 1027–1037.
786   Tupas, L., Koike, I., 1991. Simultaneous uptake and regeneration of ammonium by mixed
787   assemblages of heterotrophic marine bacteria. Mar. Ecol. Prog. Ser. 70, 273–282.
788   Van de Waal, D.B., Ferreruela, G., Tonk, L., Van Donk, E., Huisman, J., Visser, P.M., Matthijs,
789   H.C.P., 2010. Pulsed nitrogen supply induces dynamic changes in the amino acid
790   compositionand microcystin production of the harmful cyanobacterium Planktothrix
791   agardhii. FEMS Microbiol. Ecol. 74, 430–438.
792   Watson, S.B., Miller, C., Arhonditsis, G., Boyer, G.L., Carmichael, W., Charlton, M.N.,
793   Confesor, R., Depew, D.C., Höök, T.O., Ludsin, S.A., Matisoff, G., McElmurry, S.P.,
794   Murray, M.W., Peter Richards, R., Rao, Y.R., Steffen, M.M., Wilhelm, S.W., 2016. The re-
795   eutrophication of Lake Erie: Harmful algal blooms and hypoxia. Harmful Algae 56, 44–66.
796   Welschmeyer, N.A., 1994. Fluorometric analysis of chlorophyll a in the presence of chlorophyll
797   b and pheopigments. Limnol. Oceanogr. 39, 1985–1992.
798   Xie, L., Xie, P., Li, S., Tang, H., Liu, H., 2003. The low TN: TP ratio, a cause or a result of
799   Microcystis blooms?. Water Res. 37, 2073–2080.
800   Xu, H., Paerl, H.W., Qin, B., Zhu, G., Hall, N.S., Wu, Y., 2015. Determining critical nutrient
801   thresholds needed to control harmful cyanobacterial blooms in eutrophic Lake Taihu,
802   China. Environ. Sci. Technol. 49, 1051–1059.
803   Yang, J., Gao, H., Glibert, P.M., Wang, Y., Tong, M., 2017. Rates of nitrogen uptake by
804   cyanobacterially-dominated assemblages in Lake Taihu, China, during late summer.
805   Harmful Algae 65, 71–84.
806   Yin, G., Hou, L., Liu, M., Liu, Z., Gardner, W.S., 2014. A novel membrane inlet mass
807   spectrometer method to measure $^{15}NH_4^+$ for isotope-enrichment experiments in aquatic
808   ecosystems. Environ. Sci. Technol. 48, 9555–9562.
809   Zevenboom, W., de Groot, G.J., Mur, L.R., 1980. Effects of light on nitrate-limited Oscillatoria
810   agardhii in chemostat cultures. Arch. Microbiol. 125, 59–65.
811   Zevenboom, W., Mur, L.R., 1981. Simultaneous short-term uptake of nitrate and ammonium by
812   Oscillatoria agardhii grown in nitrate-or light-limited continuous
813   culture. Microbiology 126, 355–363.
814   Zhao, M.X., Jiang, Y.L., He, Y.X., Chen, Y.F., Teng, Y.B., Chen, Y., Zhang, C.C., Zhou, C.Z.,
815   2010. Structural basis for the allosteric control of the global transcription factor NtcA by

816   the nitrogen starvation signal 2-oxoglutarate. Proc. Natl. Acad. Sci. U.S.A. 107, 12487–
817   12492.

818
819
820

Tables

Table 1. Environmental parameters and nutrient concentrations in Sandusky Bay. DO values from June were measured with a sonde deployed in the eastern outer bay (east of EC 1163). Nutrient concentrations were measured in triplicate within ± 10% error margin.

Date	Station	Temp (°C)	Dissolved Oxygen (mg L^{-1})	Chl a (µg L^{-1})	NH$_4^+$ (µM)	NO$_2^-$ (µM)	NO$_3^-$ (µM)	SRP (µM)	TP (µM)	Secchi (cm)
June 5	ODNR 4	22.2		44.2	2.57	BDL**	243	0.28	3.44	38
	ODNR 6	21.9		58.3	2.64	BDL	251	0.28	3.10	48
	ODNR 2	21.7	9.18†	48.1	2.43	BDL	101	0.13	3.03	38
	Bells	ND*		5.8	2.57	BDL	62.1	0.13	2.50	ND
June 26	ODNR 4	21.5		107	2.57	BDL	33.6	0.25	9.69	32
	ODNR 6	21.7		88.8	2.71	BDL	96.4	0.28	6.47	40
	ODNR 2	21.5	9.29†	60.7	2.57	BDL	35.7	0.16	4.78	32
	Bells	20.4		44.8	2.93	BDL	41.4	0.19	1.38	106
July 31	ODNR 4	23.5		167	3.36	2.14	58.6	0.50	4.91	ND
	ODNR 6	23.6		172	2.14	4.29	77.1	0.25	4.09	ND
	ODNR 2	24.2	9.71	136	2.57	2.86	69.3	0.31	3.47	ND
	Bells	24.5		13.1	1.29	0.71	15.7	0.28	1.00	ND
August 14	ODNR 4	23.6		61.0	3.64	BDL	BDL	0.59	6.22	34
	ODNR 6	23.5		59.4	2.71	BDL	BDL	0.47	6.22	44
	ODNR 2	23.7	9.57	57.9	1.71	BDL	BDL	0.43	4.25	54
	Bells	24.4		11.2	2.79	0.71	1.43	0.38	1.16	80
August 28	ODNR 4	22.3		56.7	0.71	BDL	BDL	0.88	7.81	30
	ODNR 6	22.2		59.5	1.00	BDL	BDL	0.31	5.56	34
	ODNR 2	22.7	8.67	31.3	1.36	BDL	1.43	0.31	4.78	38
	Bells	23.1		14.9	0.86	BDL	0.71	0.31	1.53	132

*ND – not determined
**BDL – below the detection limit
† Measured east of EC 1163

Table 2. Environmental parameters and nutrient concentrations in Maumee Bay. Nutrient concentrations were measured in triplicate within ± 10% error margin.

Date	Station	Temp (°C)	Dissolved Oxygen (mg L^{-1})	Chl *a* (µg L^{-1})	NH_4^+ (µM)	NO_2^- (µM)	NO_3^- (µM)	OP (µM)	Secchi (cm)
July 17	WE6	24.6	5.21	3.50	6.29	5.13	400	4.32	20
August 9	MB18	23.9	9.18	NM	0.99	1.51	96.5	0.16	NM
August 14	WE6	25.1	10.7	532	0.33	1.46	122	0.53	20
October 10	WE6	20.7	6.00	40.9	BDL	0.02	0.40	0.17	50

*ND – not determined

Table 3. Spearman correlation for nonparametric data in Sandusky Bay.

		NH_4^+	NO_2^-	NO_3^-	SRP	TP	Temp	DO	Chl *a*	Secchi
Uptake Light	Spearman's Rho	-0.162	-0.252	**-0.561**	**0.524**	**0.874**	-0.2	-0.4	**0.597**	**-0.812**
	p value	0.5	0.3	**0.02**	**0.0**	**<0.001**	0.5	0.2	**0.01**	**0.002**
Uptake Dark	Spearman's Rho	-0.283	-0.232	**-0.64**	**0.493**	**0.766**	-0.092	-0.132	0.464	-0.493
	p value	0.3	0.4	**0.007**	**0.05**	**0.001**	0.7	0.6	0.07	0.1
Regeneration	Spearman's Rho	-0.256	-0.298	**-0.521**	0.438	**0.857**	-0.228	-0.271	**0.517**	**-0.735**
	p value	0.3	0.3	**0.04**	0.09	**<0.001**	0.4	0.6	**0.04**	**0.009**

Table 4. Comparison of Sandusky River N loading (weekly ranges and weekly averages; mT = metric ton) to NH_4^+ regeneration (station range and average for ODNR 2, 4, 6) in the summer of 2017.

Sampling Date	TN load$_w$ (mT d^{-1})	TN load$_a$ (mT d^{-1})	TKN load$_w$ (mT d^{-1})	TKN load$_a$ (mT d^{-1})	TKN/TN$_a$	Reg. NH_4^+ $_d$ (mT)	Reg. NH_4^+ $_s$ (mT)	Reg./TN$_w$	Reg./TKN$_w$
June 5th	7.8–55.6	21.1	0.3–2.46	1.23	0.132	25.3–64.9	40.7	1.9	33.0
July 31st	0.9–3.1	1.73	0.29–1.05	0.54	0.318	39.7–84.9	65.2	37.7	121
August 14th	0.17–0.40	0.257	0.16–0.23	0.194	0.840	99.8–141	123	478	633
August 28th	0.11–0.19	0.167	0.11–0.17	0.145	0.919	186–218	199	1190	1375

w – weekly range
a – weekly average
d – station range for sampling on date
s – station average for sampling on date

Figure List

Figure 1. Map of sampling locations in Sandusky Bay (41.46883; -82.85299) and Maumee Bay (41.71516; -83.39496). The inset shows the location of the western basin relative to the rest of Lake Erie.

Figure 2. Ammonium regeneration and potential uptake rates in Sandusky Bay in 2017. Potential light uptake rates (A), potential dark uptake rates (B), and averaged regeneration rates (C). Values are averaged (three replicates) with error bars showing ± one standard error.

Figure 3. Community Biological Ammonium Demand (CBAD) in Sandusky Bay in light (A) and dark (B). Values are averaged (three replicates) with error bars showing ± one standard error.

Figure 4. Michaelis-Menten NH_4^+ uptake kinetics in Sandusky Bay (A) and Maumee Bay (B) in 2017. The Michaelis–Menten model fits for Sandusky Bay were: June 5 (r = 0.98), June 26 (r = 0.75), July 31 (r = 0.92), Aug 14 (r = 0.73), Aug 28 (r = 0.97), and Maumee Bay model fits were: July 17 (r = 0.38), Aug 9 (r = 0.98), Aug 14 (r = 0.96), Oct 10 (r = 0.98).

Figure 5. Metatranscriptome data and ambient NH_4^+ and NO_3^- concentrations in Sandusky Bay in 2015. *cphA1* and *cphA2* are *Planktothrix agardhii* paralogs encoding cyanophycin synthetase, *cphB* encodes cyanophycinase, and *glnA* and *amt* encode glutamine synthetase and NH_4^+ transporters. Relative transcript abundance is presented as reads per kilobase of transcript per million mapped reads (RPKM).
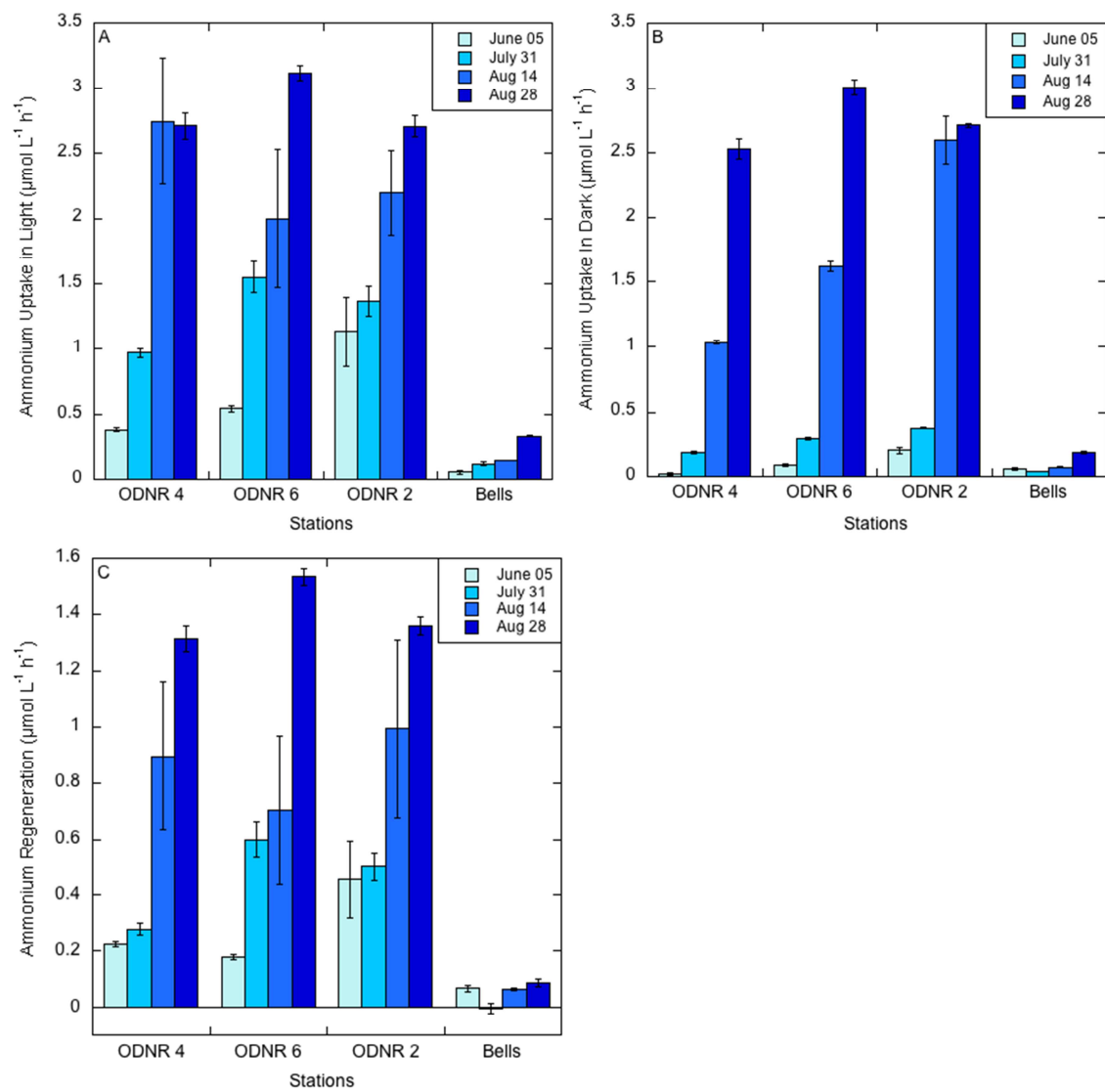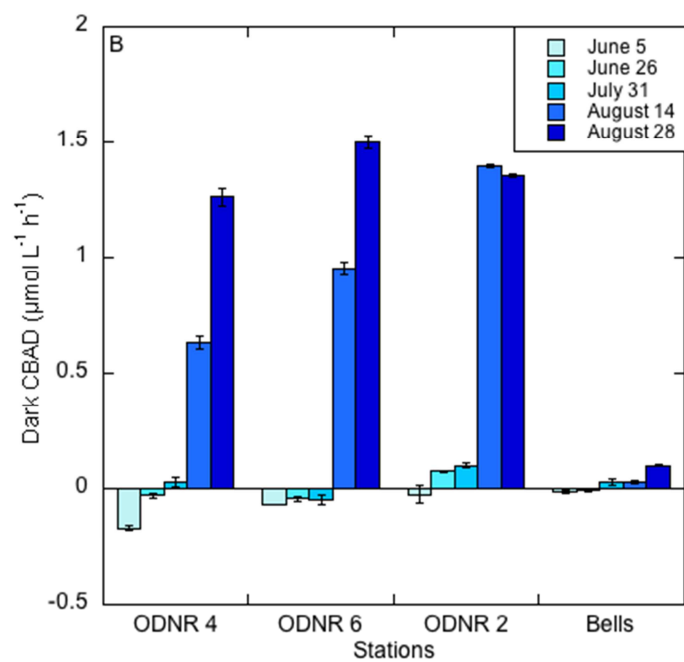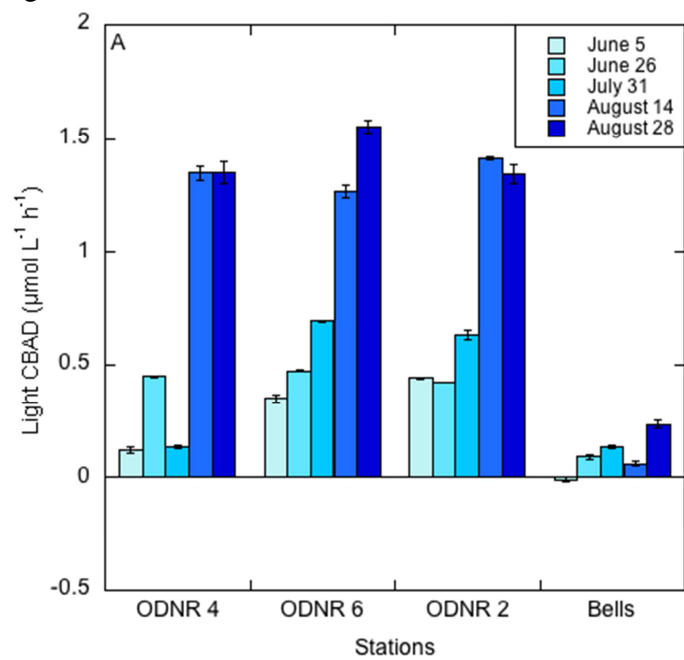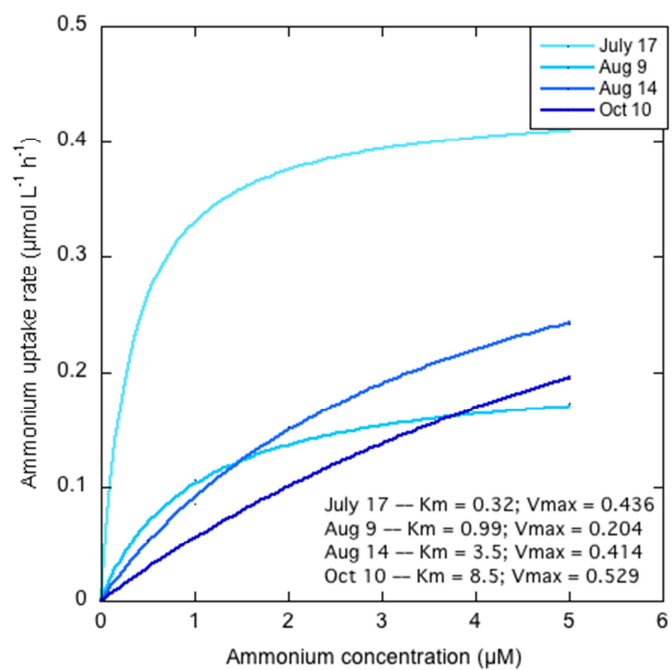
Figures

Figure 1

Figure 2

Figure 3

Figure 4

Figure 5.